APPLIED AND ENVIRONMENTAL MICROBIOLOGY, Mar. 1983, p. 1066–1084
0099-2240/83/031066-19$02.00/0

Vol. 45, No. 3

Microbial Fouling of Reverse-Osmosis Membranes Used in Advanced Wastewater Treatment Technology: Chemical, Bacteriological, and Ultrastructural Analyses

H. F. RIDGWAY,† A. KELLY, C. JUSTICE, AND B. H. OLSON*

Program in Social Ecology, Environmental Analysis Division, University of California, Irvine, California 92717

Received 10 September 1982/Accepted 29 December 1982

Biofouling of reverse-osmosis membranes was investigated at an advanced wastewater treatment facility. Cellulose diacetate membranes operated for approximately 4,000 h became uniformly coated with a mucilaginous fouling layer. The fouling material was approximately 93% water by weight, and nearly 90% of the dehydrated residue was organic in composition. Calcium, phosphorous, sulfur, and chlorine were the major inorganic constituents detected. Protein and carbohydrate represented as much as 30 and 17%, respectively, of the dry weight of the biofilm. Bacteriological plate counts indicated up to 5.6×10^6 CFU/cm^2 of membrane surface. Accumulation of [^{3}H]glucose in the biofilm and measurement of ATP indicated that the fouling bacteria were metabolically active in situ. The genus *Acinetobacter* and the *Flavobacterium-Moraxella* group were the major generic groups associated with the feedwater surface of the membrane, whereas species of the generic groups *Acinetobacter, Pseudomonas-Alcaligenes*, and *Bacillus-Lactobacillus* predominated on the permeate water surface. Electron microscopy revealed that the biofilm on the feedwater surface of the membrane was 10 to 20 μm thick and was composed of several layers of compacted bacterial cells, many of which were partially or completely autolyzed. The bacteria were firmly attached to the membrane surface by an extensive network of extracellular polymeric fibrils. Polyester (Texlon) support fibers located on the permeate surface of the reverse osmosis membranes were sparsely colonized, suggesting bacterial regrowth in the product water collection system.

As present and anticipated shortages of potable water supplies become more acute, especially in the arid southwestern region of the United States, treatment facilities for the large-scale reclamation of contaminated wastewaters are receiving increasing attention. In recent years, there has been extensive research into advanced wastewater treatment technologies such as granular activated carbon adsorption for the removal of organochlorine derivatives (28) and reverse osmosis (RO) for demineralizing brackish waters (2, 3, 13, 22, 27–31, 34).

Recent technological advances in the design and manufacture of polyamide, cellulose acetate, and composite-polymer semipermeable membranes for a variety of commercial purposes have made RO the preferred method for the efficient recovery of high-purity water directly from raw, chemically contaminated, or brackish water resources receiving a minimum of pretreatment. In the RO process utilized at Water Factory 21, a 0.66-m^3/s advanced wastewater treatment facility in Southern California, pretreated wastewater is forced under high pressure (about 500 lb/in^2; 35 kg/cm^2) through a three-pass series of spiral-wound cellulose diacetate semipermeable membranes. These anisotropic membranes function like molecular sieves to remove nearly all suspended colloidal substances (including bacteria and viruses) and 90 to 98% of the dissolved inorganic and organic constituents present in the water supply.

The economic feasibility of the RO process depends critically on maintaining a constant permeate (product) water flux across the membrane. The water flux (F_w) and salt flux (F_s) of semipermeable RO membranes can be expressed mathematically by the general equations (2, 29, 30, 35) $F_w = -A(\Delta P - \Delta\pi)$ and $F_s = -B(\Delta C_{ss})$, where A and B represent the membrane and solute permeation constants, respectively; ΔP and $\Delta\pi$ are the differences in the applied and osmotic pressures, respectively, across the RO membrane; and ΔC_{ss} is the difference in the concentrations of dissolved salts on the two

† Current address: Orange County Water District, Fountain Valley, CA 92708-0300.

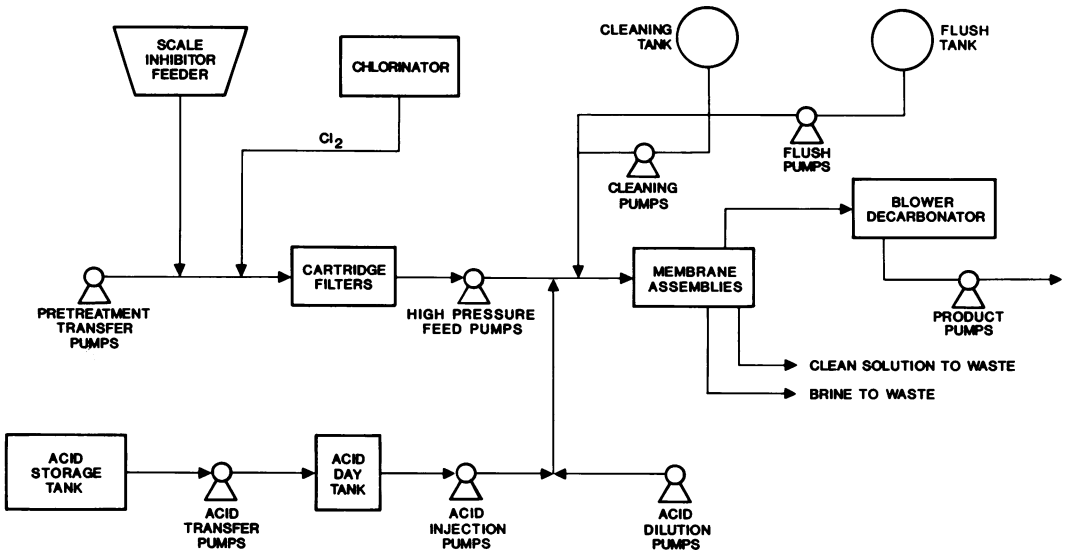

FIG. 1. Schematic flow diagram of RO facility at Water Factory 21.

sides of the membrane. Whereas F_w is a pressure-dependent diffusional process, F_s is essentially independent of the applied pressure. Hence, the desalination factor (the quotient of solute concentration in the feedwater divided by solute concentration in the permeate water) may be significantly increased at the elevated barometric pressures which are characteristically employed in the RO process.

The net water flux can be dramatically influenced not only by the permeation design characteristics of the semipermeable membrane itself but also by membrane compaction occurring when the membrane is initially exposed to increased pressure and by the gradual accumulation of substances on the membrane surface which can reduce turbulent mixing and impede the molecular diffusion of water. Because RO is a highly energy-dependent process, the gradual increase in membrane flux decline which results from fouling can significantly increase plant operating expenditures. Although the RO membranes can be periodically cleaned with certain chelating agents and detergent compounds which may partially restore flux (29, 35), the accumulation of fouling material eventually necessitates the premature replacement of the membranes.

Membrane fouling substances may include hydrated metallic oxides, calcium, barium and strontium precipitates, simple and complex colloids, organic slimes, and aluminum and silica deposits (2, 29, 30). In addition, numerous investigators have shown that a variety of microorganisms is present on the surfaces of RO membranes after prolonged operation (2, 29, 30). It is widely believed that the development of a microbial biofilm may contribute significantly to a decline in water flux and a deterioration of overall membrane performance (e.g., loss of mineral rejection). However, the precise relationship between flux decline and microbial fouling is not completely understood, and few detailed descriptions of the specific chemical and microbiological properties of the biofilm have appeared in the literature (29).

In an effort to obtain more precise and comprehensive knowledge of the chemical constitution, microbial ecology, and ultrastructure of the membrane fouling layer, the surfaces of cellulose diacetate RO membranes installed at Water Factory 21 were investigated by scanning and transmission electron microscopy, energy dispersive X-ray (EDX) microanalysis, and a variety of biochemical and microbiological techniques. The results of these investigations are discussed in this report.

MATERIALS AND METHODS

Description of RO facility. A schematic flow diagram of the 0.22-m^3/s RO facility at Water Factory 21 is depicted in Fig. 1. The feedwater for the RO assembly consists of secondary (activated sludge) treated municipal effluent from the Orange County Sanitation District. This water is pretreated by a variety of chemical and biological processes, including lime clarification, ammonia air stripping, recarbonation, mixed media filtration, and granular activated carbon adsorption. Immediately before RO, the wastewater is further treated by adding sodium hexametaphosphate as an inorganic scale-precipitation inhibitor and 0.5 mg of chlorine per liter for partial control of microbial growth within the RO membrane modules. The water

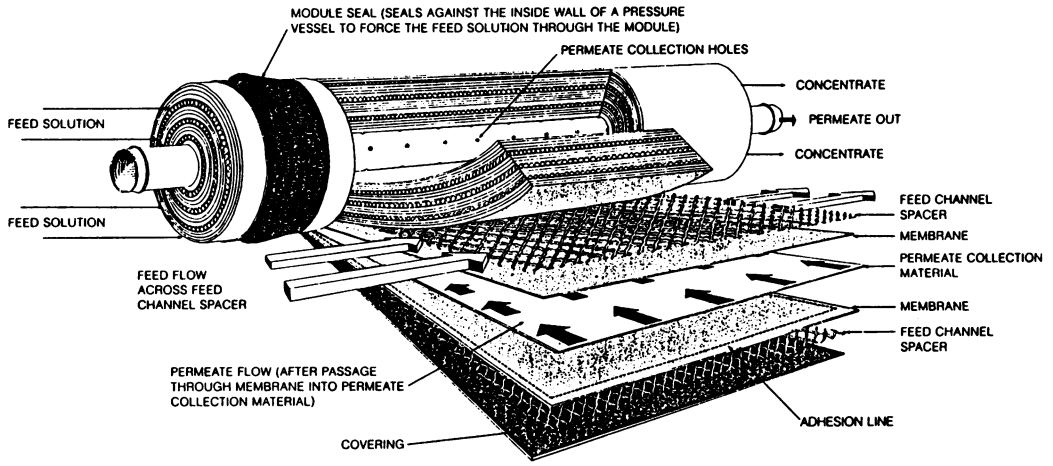

FIG. 2. Schematic illustration depicting construction details of a spirally wound RO module (type HR-8150). The module measures 8 in. in diameter by 36 in. in length (about 20 by 91 cm).

is then passed through a series of 25-μm cartridge filters for removal of suspended particulate matter and is pressurized by two vertical turbine feed pumps to a dynamic head of approximately 480 lb/in^2 (33.8 kg/cm^2). Sulfuric acid is injected into the high-pressure feed header to adjust the pH to approximately 5.5 before the water is applied to the RO membranes. The demineralized water receives posttreatment in two packed-tower decarbonators which air strip dissolved carbon dioxide resulting from the pH adjustment to 5.5. The decarbonators also remove volatile trace organic compounds.

The individual RO membrane elements measure approximately 8 in. in diameter by 36 in. in length (20 by 91 cm) and are of the spiral-wound configuration (Fluid Systems, UOP, Inc., Des Plaines, Ill.). A schematic illustration showing the construction details of a single spiral-wound element (Fluid Systems type HR-8150) is presented in Fig. 2. The pretreated wastewater is fed longitudinally across a series of 18 cellulose diacetate membrane envelopes rolled concentrically about a polyvinyl chloride permeate water collection tube. A diagrammatic cross section of a single membrane envelope is shown in Fig. 3. The feedwater flow is vectorial, having both horizontal and perpendicular flow components with respect to the RO membrane surface. Each membrane envelope in an element is separated from adjacent envelopes by a plastic mesh feedwater channel spacer (Vexar spacer). The semipermeable portion of the cellulose diacetate membrane, which is approximately 0.2 μm thick, is supported by a layer of straight woven polyester Texlon fibers on the permeate surface of the membrane. A total of 1,500 spiral-wound elements are assembled in a three-pass series in which the brine water (or concentrate) generated by the initial bank of elements (first-pass membranes) is fed into a second bank of elements (second-pass membranes) and the concentrate from the second-pass elements is fed into a third and final bank of elements (third-pass membranes). The RO plant is designed to provide 90% salt removal while achieving 85% water recovery.

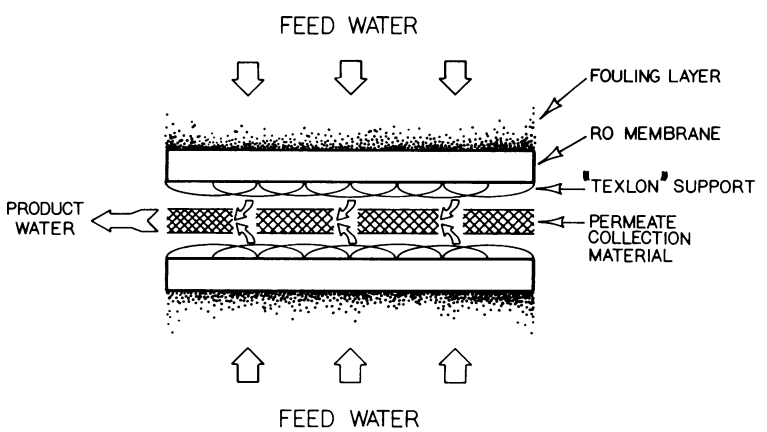

FIG. 3. Cross section of a single membrane envelope showing accumulation of fouling material.

Sampling procedures. First-pass, second-pass, and third-pass elements which had been in more or less continuous operation for approximately 4,000 h were removed from the RO assembly on 27 January 1981. The elements were dismantled and returned to the laboratory, where the mucilaginous fouling material which had accumulated on the feedwater surfaces of the membranes was scraped off asceptically for chemical and bacteriological analysis. In addition, small sections of membranes were excised for electron microscopy as described below.

Bacterial enumeration and taxonomic identification. Fresh biofilm scrapings were dispersed aseptically into 0.3 mM potassium phosphate buffer containing 1.0 mM $MgSO_4$ (1). Serial dilutions were prepared, and appropriate samples were filtered in duplicate through mixed-ester cellulose membrane filters (pore size, 0.2 μm; type GN6; Gelman Sciences, Inc., Ann Arbor, Mich.). The filters were placed on m-SPC (28a) and R-2A (D. J. Reasoner and E. E. Geldreich, Abstr. Annu. Meet. Am. Soc. Microbiol. 1979, N7, p. 180) media and were incubated for 96 h at 28°C. Colonies were counted and transferred to slants of the same medium for taxonomic identification.

Bacteria associated with the permeate surface of the RO membranes were recovered by momentarily pressing square portions of the membranes (about 2 by 2 cm) onto the surfaces of m-SPC and R-2A plates. Colonies which developed after incubation at 28°C for 96 h were assumed to have arisen from cells dislodged from the permeate surface of the membrane. These colonies were counted and transferred to agar slants of the same medium for subsequent identification.

Gram-negative, rod-shaped bacteria were identified to the genus level by a modification of the rapid three-tube fermentation test described by Lassen (18). The Lassen procedure was modified by substituting Kligler iron agar (Difco Laboratories, Detroit, Mich.) for the combined lactose-glucose-H_2S medium. Additional biochemical tests were occasionally performed with the API-20 enteric identification system (Analytab Products, Plainview, N.Y.). Gram-positive microorganisms were identified by characteristics outlined in *Bergey's Manual* (4).

Chemical analyses. General mineral analyses of the RO membrane fouling layers were performed according to *Standard Methods* (1) by the Orange County Water District Laboratory. The amount of protein in the fouling layer was determined by the method of Lowry et al. (19) with bovine serum albumin as the standard. Total carbohydrate was quantitatively measured by the phenol-sulfuric method of Dubois et al. (10) with a glucose standard. The concentration of intracellular ATP was determined by the method described by Hamilton and Holm-Hansen (14). Samples were extracted by boiling for 4.5 min in 5.0 ml of 20 mM Tris buffer (pH 7.6), transferred to a water bath at 23°C, and frozen at −70°C until analysis. The ATP in the extracts was measured by the luciferin-luciferase assay of Holm-Hansen and Booth (15) with a Packard Picolite Luminometer.

Scanning electron microscopy. Upon dismantling the spiral-wound RO modules, square portions of membrane approximately 1 by 1 cm were immersed in an ice-cold solution of 2.5% (vol/vol) glutaraldehyde in 10 mM monobasic potassium phosphate buffer, pH 7.0. The membrane samples were removed from areas immediately adjacent to where samples were obtained for bacteriological and chemical analyses. After overnight fixation at 4°C, the membrane fragments were consecutively washed three times in distilled water, dehydrated in an increasing ethanol concentration series and a Freon 113-ethanol concentration series, and critical point dried by the method of Cohen et al. (9) with absolute Freon 13 as the intermediate transitional fluid. The dried membranes were sliced into short strips 1 or 2 mm wide. The strips were mounted on aluminum stubs with conducting silver paint, coated with gold-palladium (60:40), and examined in a Hitachi model S 500 scanning electron microscope (SEM) operated at 15 keV with a working distance of 10 mm and a stage tilt angle of 0°. Black and white photographs were made on Polaroid type P/N55 film.

SEM-EDX microanalysis. Square sections of membrane measuring approximately 1 cm on a side were air dried without prior fixation and were mounted on aluminum stubs with a colloidal graphite suspension. The Texlon support matrix was stripped from the permeate surface of the membrane before drying and mounting to reduce specimen curling. The mounted membrane samples were coated with a layer of evaporated carbon and examined in a Cambridge model S4 SEM operated at 30 keV and equipped with an EDX unit (EG&G Ortec, Oak Ridge, Tenn.). A continuous X-ray energy spectrum from 0 to 10 keV was integrated over a minimum of 200 s for each elemental scan. The K, L, and M X-ray energy lines were utilized for identifying the elements present in the samples. Control elemental scans were performed on both the naked aluminum stub surface and on stubs coated with the colloidal graphite suspension. Specimens were quantified by normalizing the corrected areas under the peaks for the elements of interest with the Ortec inboard computer system and standard software supplied by the manufacturer.

Transmission electron microscopy. Small fragments of fouled RO membrane were immersed overnight in ice-cold 2.5% (vol/vol) glutaraldehyde prepared in 10 mM monobasic potassium phosphate buffer, pH 7.0. The membranes were then washed in two changes of phosphate buffer, suspended in 1.0% (wt/vol) osmium tetroxide in phosphate buffer, and fixed at 0 to 2°C for 2 h. The osmium-fixed membranes were washed twice in distilled water and dehydrated at room temperature (23°C) in graded ethanol and propylene oxide concentration series. The cellulose diacetate membranes dissolved in the propylene oxide solutions, leaving the intact biofilm apparently undisturbed. The dehydrated biofilms were infiltrated, embedded in Lufts Epon, and polymerized at 60°C for 2 days. Thin sections were prepared on a Sorvall MT-2B ultramicrotome, mounted on Formvar-carbon-coated, open-mesh, copper grids, and poststained with 2.0% (wt/vol) aqueous uranyl acetate followed by Reynolds lead citrate (24). Specimens were examined in a Zeiss model EM-9S transmission electron microscope operated at an accelerating voltage of 60 keV.

RESULTS

Visual inspection of fouled membranes. The feedwater surfaces of the first-, second-, and third-pass membranes were uniformly coated with a gray-black mucilaginous substance (Fig.

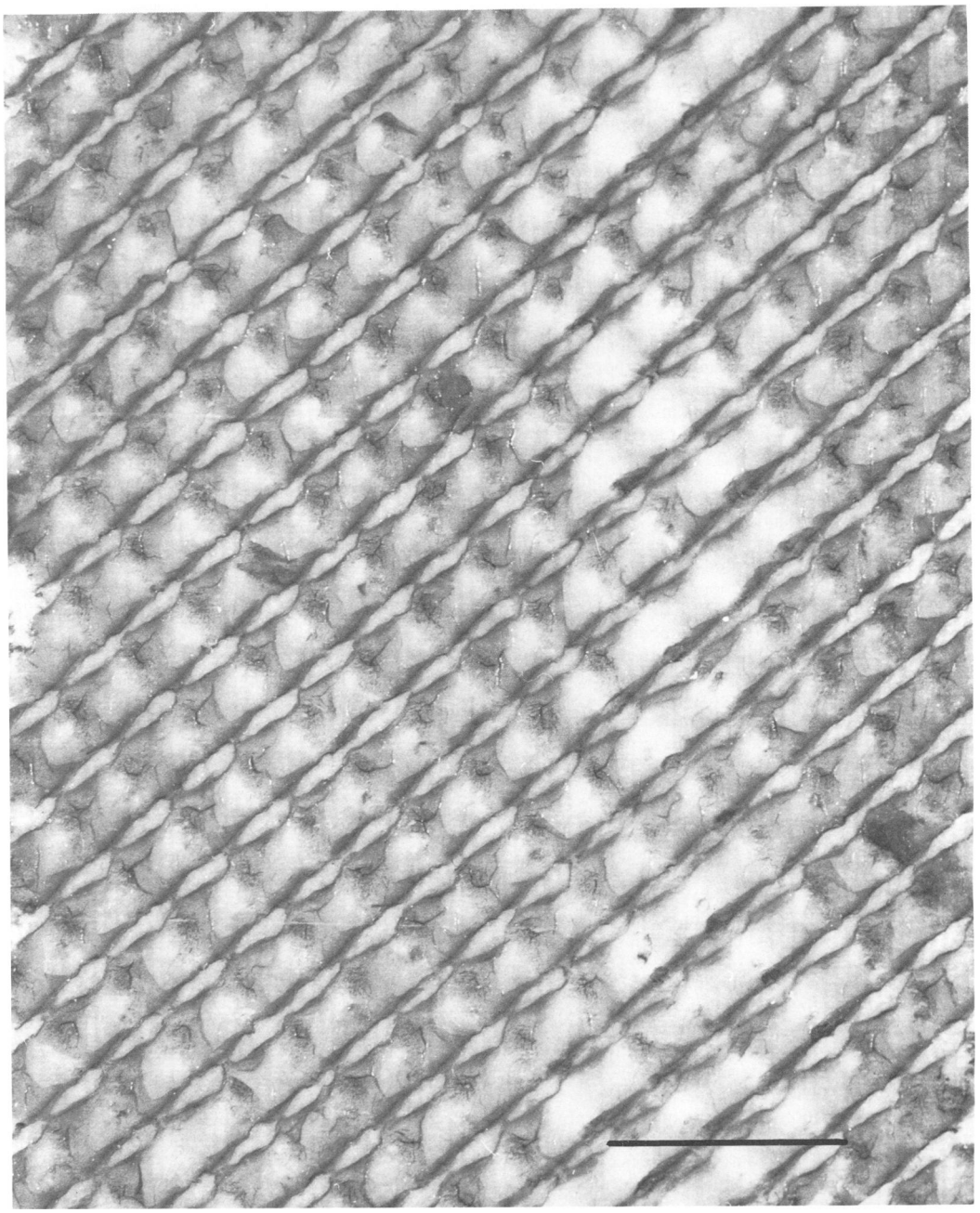

FIG. 4. Close-up photograph showing criss-cross pattern of biofilm on feedwater surface of second-pass RO membrane. Bar, 1.0 cm.

4). The fouling layers on all three membrane passages appeared similar, each exhibiting a regular criss-cross pattern which was congruent with the pattern of the overlying plastic feedwater channel spacer (Vexar) which separates adjacent membrane envelopes in the intact RO element (see Fig. 2). The fouling substance, which had a slippery, gel-like texture, could be readily scraped or washed from the cellulose diacetate membrane surfaces. Visual inspection of the permeate water surfaces of these membranes (i.e., the surfaces of the Texlon support fibers) revealed little or no evidence of inorganic scale formation or microbiological fouling.

Chemical analysis of fouling material. Although visually there appeared to be somewhat less foulant associated with the third-pass membrane, gravimetric analysis indicated that the actual amount of fouling material (expressed as the wet weight of crude foulant scrapings per unit of membrane surface area) increased noticeably from the first-pass to the third-pass membrane (Table 1). Approximately 93% of the biofilm weight consisted of water, and nearly 90% (wt/wt) of the dehydrated residue (60°C, 24 h) was found to be volatile upon incineration at 550°C. This volatile fraction was regarded as primarily organic. Nonvolatile inorganic substances represented approximately 10% (wt/wt) of the dehydrated residue. Calcium, chlorine, sulfur, and phosphorous (in decreasing order of concentration) were the major inorganic constituents present in the biofilm from all three membrane passages. Trace quantities of potassium, aluminum, iron, chromium, copper, and silicon were also detected. Most of the elements detected increased from the first-pass to the third-pass membrane. These observed increases in the amounts of the individual inorganic species may reflect their increasing concentrations in the feedwater as it progresses from the first-pass to the third-pass membrane. Chromium was the only element which exhibited a decline in concentration from the first-pass to the third-pass membrane. It is possible that chromium may be selectively removed from the feedwater by binding to the first-pass membrane or to organic or inorganic substances which accumulate on the membrane surface.

Because of the high organic content of the biofouling material, it was of interest to determine the amounts of protein and carbohydrate substances present in the samples. The first-, second-, and third-pass membranes were found to contain approximately 15, 24, and 30% (dry weight) protein, respectively (Table 1). The total carbohydrate accounted for approximately 13 to 17% of the dry weight. These data indicate that large quantities of biologically synthesized macromolecules constitute a major proportion of the biofilm layers.

SEM-EDX analysis of fouled membranes. The above inorganic chemical analyses were corroborated and extended by the SEM-EDX technique. A continuous X-ray energy spectrum for a second-pass RO membrane is shown in Fig. 5, and the quantitative analytical data for all the membrane passages are presented in Table 2. In addition to most of the elements detected by conventional chemical analysis, trace quantities of sodium, magnesium, titanium, and iodine were also detected by the SEM-EDX procedure.

A discrepancy existed between the percentage composition of the inorganic fraction as deter-

TABLE 1. Chemical analysis of biofilm scrapings from RO membranes[a]

Membrane	Amt of foulant (mg [wet wt]/cm²)	Moisture (% wet wt)	Total fraction		Protein	Carbohydrate	CaO	K	Al	Fe	Cr	Cu	Cl	SO_4	PO_4-P	NO_3-N	SiO_2
			Organic[b]	Inorganic[c]													
First-pass	8.2	93.7	92.6	7.4	15.0	13.2	1.9	0.03	0.08	0.21	0.12	0.003	0.60	0.87	0.90	0.01	<0.01
Second-pass	9.9	93.0	91.6	8.4	24.1	17.6	2.0	0.04	0.08	0.32	0.09	0.003	1.10	0.93	1.00	0.01	<0.01
Third-pass	12.6	93.9	87.3	12.7	30.1	13.2	2.65	0.06	0.08	0.35	0.05	0.003	2.40	0.90	1.40	0.01	<0.01

[a] All values show percentages of dry weight unless otherwise noted.
[b] Volatile at 550°C.
[c] Nonvolatile at 550°C.

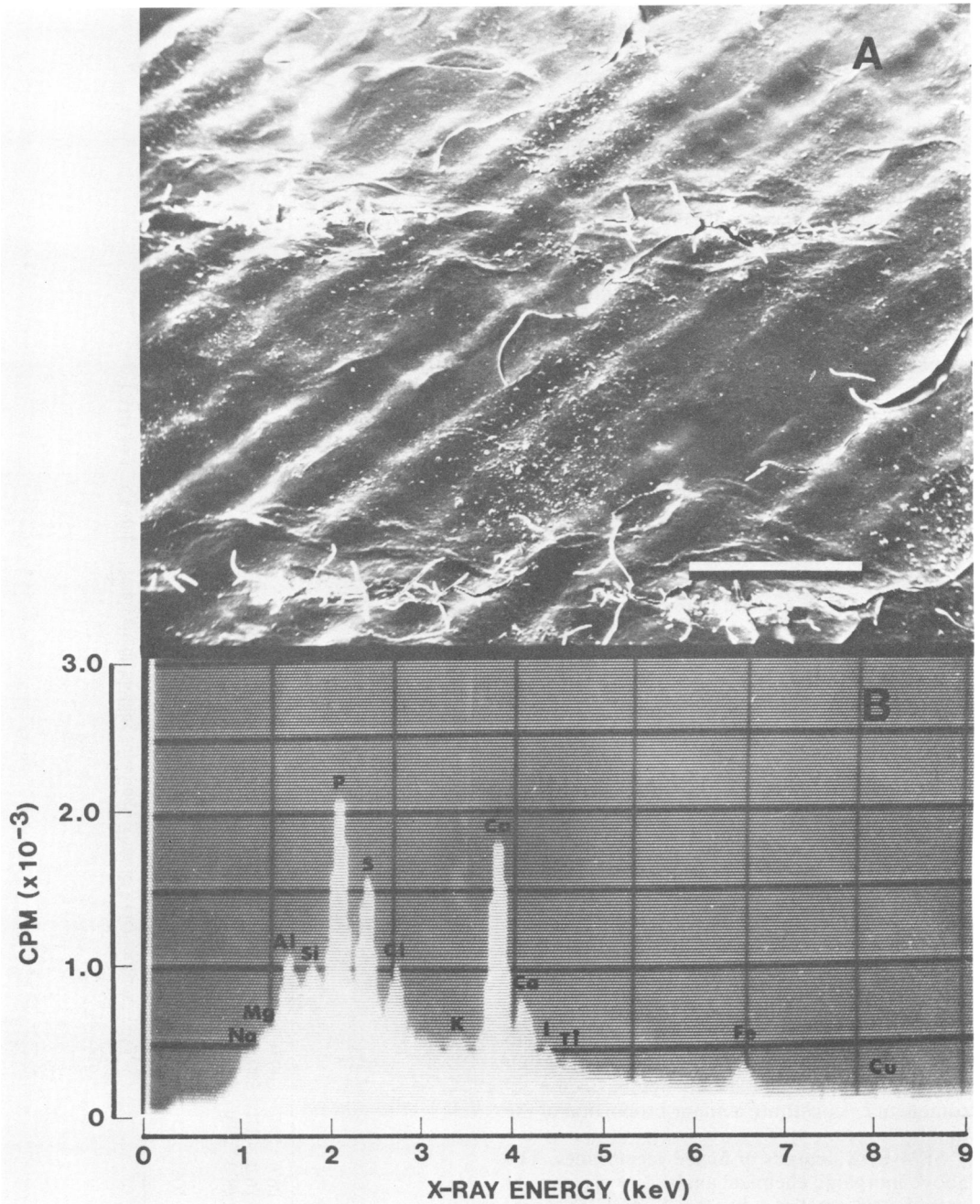

FIG. 5. (A) Portion of second-pass RO membrane: (B) continuous SEM-EDX spectrum of biofilm from the same. Peak identifications are indicated. Spectra for the first- and third-pass RO membranes appeared similar. The relatively high aluminum content may represent an artifact owing to extraneous X-ray emission from aluminum specimen preparation stub. Bar, 100 μm.

mined by conventional analytical methods and as determined by the SEM-EDX technique (Table 2). This difference may be ascribed in part to the relatively small area of biofilm analyzed by the SEM-EDX procedure (approximately 1 mm^2 or less) compared with the much larger areas (several square centimeters) analyzed by conventional chemical techniques. Furthermore,

TABLE 2. Comparison of elemental composition of biofilms as determined by SEM-EDX and chemical analysis

Element	Amt in membrane: First-pass EDX[a]	First-pass Other[b]	Second-pass EDX	Second-pass Other	Third-pass EDX	Third-pass Other
Ca	29.0	40.1[e]	31.5	35.8[e]	33.6	29.7[e]
K	NA[c]	0.65	0.28	0.73	0.98	0.68
Al	13.4	1.70	6.41	1.42	6.78	0.88
Fe	3.17	4.44	3.10	5.74	3.51	3.93
Cr	NA	2.53	NA	1.54	NA	0.53
Cu	0.62	0.06	0.69	0.05	ND	0.03
Cl	10.3	12.7	7.64	19.7	7.69	26.9
S	17.9	18.4	17.9	16.7	19.0	21.3
P	25.2	19.0[f]	28.2	17.9[f]	24.0	15.7[f]
N	NA	2.11[g]	NA	0.18[g]	NA	0.11[g]
Si	ND[d]	2.11[h]	1.65	0.18[h]	2.84	0.11[h]
I	NA	NA	1.41	NA	1.19	NA
Na	0.41	NA	0.62	NA	1.09	NA
Mg	NA	NA	0.55	NA	ND	NA

[a] Amount of element expressed as percentage of X-ray counts from all elements combined. See text for details of SEM-EDX procedure.

[b] Amount of element or compound expressed as percentage of total elements combined. Chemical analyses done according to *Standard Methods* (1).

[c] NA, Not analyzed.

[d] ND, Not detected.

[e] Expressed as CaO.

[f] Expressed as PO_4-P.

[g] Expressed as NO_3-N.

[h] Expressed as SiO_2.

the 30-keV electron beam employed in the SEM-EDX procedure may not completely penetrate the biofilm, which can be up to 20 μm thick (see below). Thus, the SEM-EDX technique may be incapable of detecting those elements which are present several micrometers beneath the surface of the biofilm.

Microbiology of fouled RO membranes. (i) Bacterial enumeration. The total numbers of CFU detected in the biofouling material scraped from the first-, second-, and third-pass membranes are shown in Table 3. The number of viable bacteria per gram (wet weight) of fouling material varied from approximately 5×10^7 for the first-pass membrane to approximately 5×10^8 for the third-pass membrane. These values correspond to about 4.2×10^5 and 5.6×10^6 CFU/cm^2 of membrane surface area, respectively. In addition, relatively high concentrations of ATP were detected in the fouling material from the second- and third-pass membranes, further indicating the presence of large numbers of viable microorganisms (the first-pass membrane was not analyzed for this parameter). The fouling bacteria were potentially metabolically active in situ since intact fragments of the biofilm actively accumulated tritium-labeled glucose, a process which was inhibited by the addition of 5.0% (vol/vol) formaldehyde (data not shown).

The viable bacteria associated with the surfaces of the Texlon support fibers on the permeate water side of the RO membrane were estimated since it was not technically feasible to scrape this side of the membrane. Instead, the number of attached cells was estimated by momentarily pressing an RO membrane section firmly onto an agar surface. Presumably, cells adhering between Texlon fibers or otherwise physically prevented from coming into direct contact with the agar surface would not be detected by this technique. Nevertheless, between 20 and 100 CFU/cm^2 of membrane surface were routinely recovered by this technique. First-, second-, and third-pass membranes gave similar results. However, these results were frequently further complicated by extensive and rapid spreading (swarming) of certain colonial

TABLE 3. Bacteriological properties of biofilm scrapings from RO membranes

Membrane	ATP (μg/g) [dry wt])	CFU/cm^2 detected with medium: m-SPC	R-2A
First-pass	NA[a]	4.8×10^5	4.2×10^5
Second-pass	337	4.2×10^6	5.3×10^6
Third-pass	69.5	3.5×10^6	5.6×10^6

[a] NA, Not analyzed.

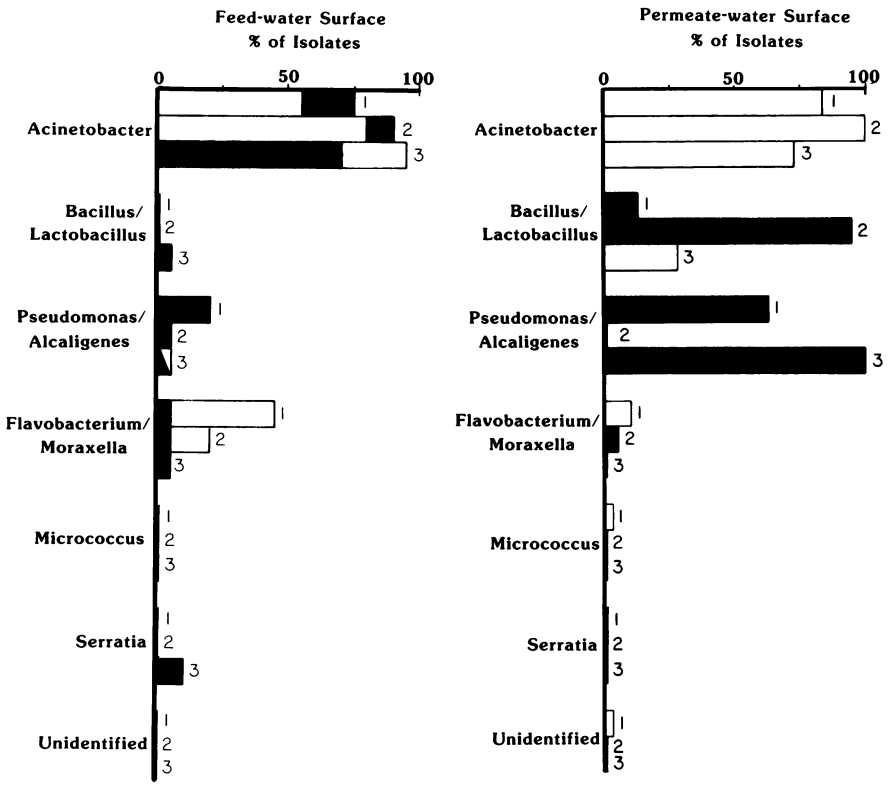

FIG. 6. Percentage of bacterial isolates (by generic group) recovered from RO membranes on low-nutrient R-2A medium (□) and m-SPC medium (■). Numbers above bars show membrane passage.

types which developed upon incubation at 28°C. Based on these observations, it was estimated that comparatively low numbers of bacteria (on the order of 100 cells per cm^2 of surface area) were associated with the permeate surface of the RO membranes. This number of cells is three to four orders of magnitude less than that found on the feedwater surfaces of the RO membranes. Subsequent examination of the permeate surfaces of the membranes in the SEM (see below) tended to substantiate this estimate, although a precise quantitative relationship between the SEM counts and the plate counts on m-SPC and R-2A media was not established in this study.

(ii) Bacterial identification. A total of 259 bacterial isolates recovered from m-SPC or R-2A media were identified from the feedwater and permeate water surfaces of the first-, second-, and third-pass RO membranes (Fig. 6). A total of six generic groups were identified: *Acinetobacter, Bacillus-Lactobacillus, Flavobacterium-Moraxella, Pseudomonas-Alcaligenes, Serratia,* and *Micrococcus*. The major bacterial genera associated with the feedwater surfaces of the membranes were *Acinetobacter* and the *Flavobacterium-Moraxella* group. Other minor genera isolated from this surface were the *Bacillus-Lactobacillus* and *Pseudomonas-Alcaligenes* groups and the genus *Serratia*. The genus *Acinetobacter* was likewise the predominant genus recovered from the permeate water (Texlon fiber) surfaces of the RO membranes. The *Bacillus-Lactobacillus* and *Pseudomonas-Alcaligenes* groups were also present in relatively high numbers. However, the *Flavobacterium-Moraxella* group and the genus *Micrococcus* were found only in comparatively low numbers on the permeate side of the RO membranes.

Some differences in the composition of the microbial flora were observed among the first-, second-, and third-pass membranes. For example, the *Pseudomonas-Alcaligenes* group of microorganisms was readily detected on the permeate water surfaces of the first-pass and third-pass membranes but not the second-pass membranes.

A comparison of the low-nutrient R-2A medium and the m-SPC medium, indicated some selectivity in the kinds of microorganisms recovered. For example, *Acinetobacter* spp. were only recovered from the permeate water surfaces of the RO membranes with the R-2A

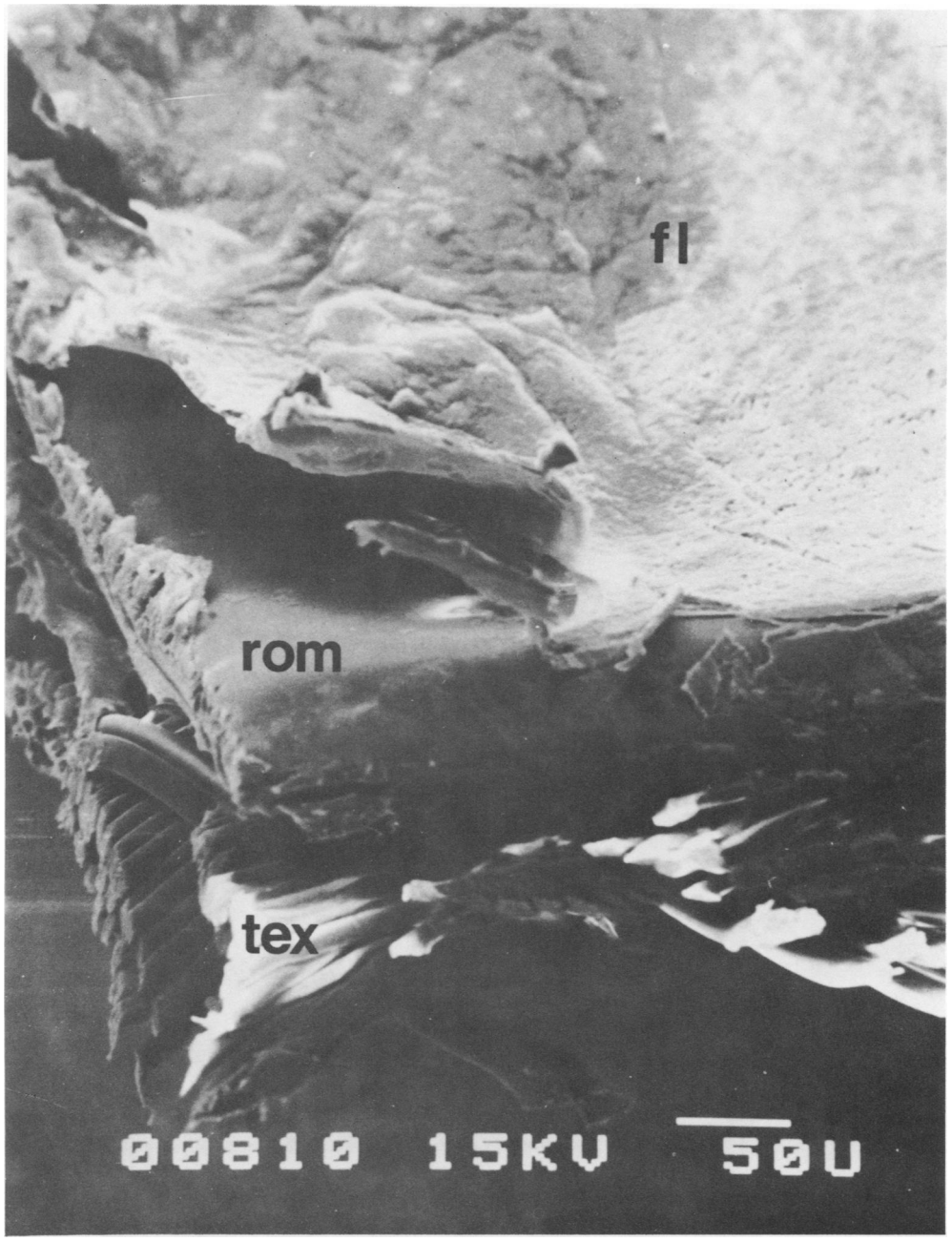

FIG. 7. Low-magnification SEM micrograph showing construction of second-pass RO membrane. Symbols: fl, fouling layer on feedwater side of membrane; rom, surface of cellulose diacetate membrane; tex, polyester Texlon support fibers on permeate side of membrane. Bar, 50 μm.

medium. However, roughly equal numbers of *Acinetobacter* spp. were recovered from the feedwater surfaces of the membranes with both types of growth media. Moreover, the R-2A medium appeared to be superior for the recovery of the *Flavobacterium-Moraxella* group and inferior for the recovery of the *Pseudomonas-Alcaligenes* group. These data should be interpreted cautiously, however, since the total number of bacteria isolated in each case was low (30 to 50) and not amenable to rigorous statistical evaluation.

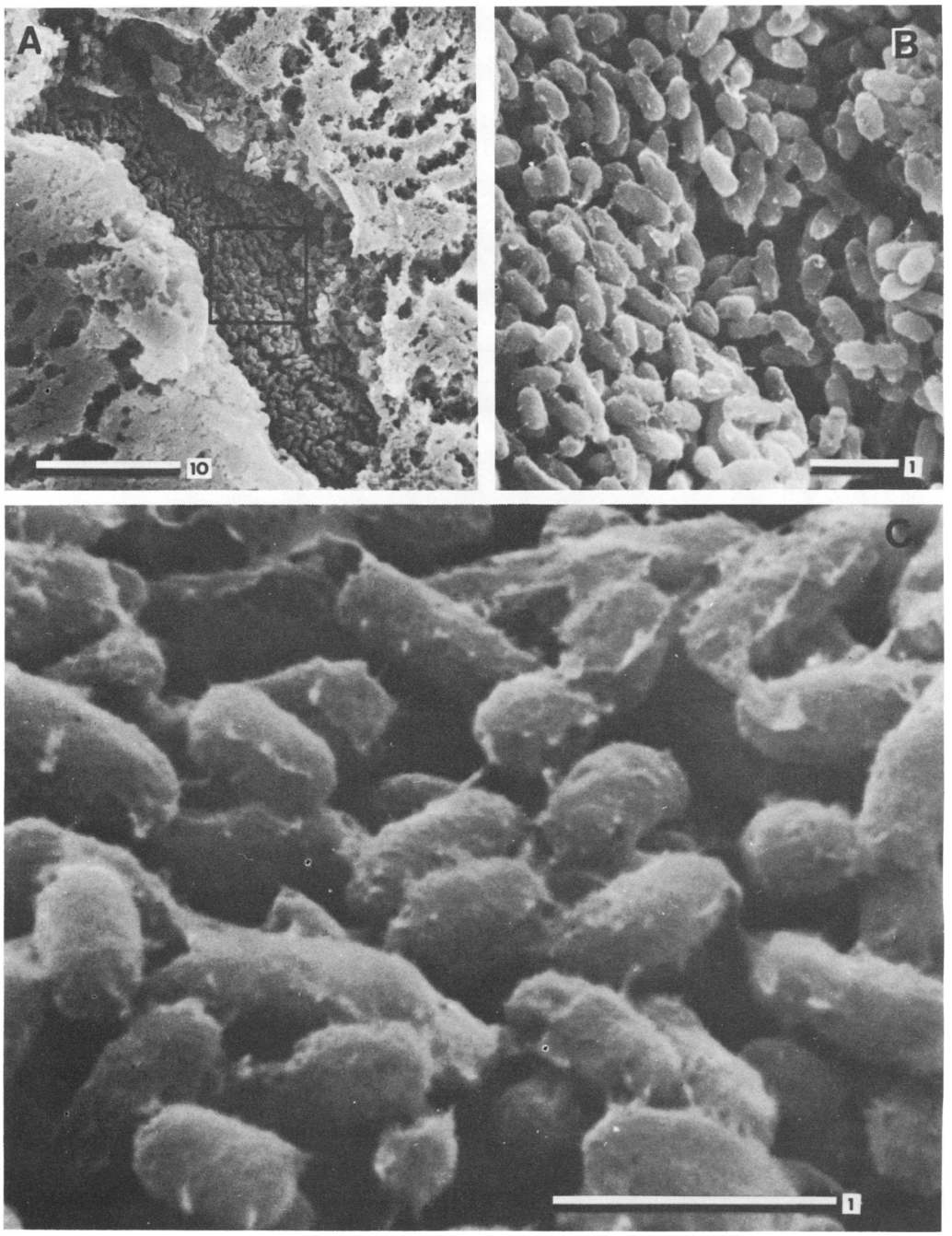

FIG. 8. Scanning electron micrographs of feedwater surface of second-pass RO membrane showing biofilm at progressively higher magnifications. Note extracellular fibrillar material associated with individual bacterial cells in C. First- and third-pass membranes appeared similar. Bars, 10 (A) and 1 (B, C) μm.

Ultrastructure of fouled RO membranes. (i) SEM analysis of fouled membranes. Figure 7 shows a low-magnification scanning electron micrograph of the fouled first-pass RO membrane. Owing to a drying artifact, the fouling layer (fl in the figure) separated from the actual feedwater surface of the RO membrane (rom). The straight woven polyester Texlon support fibrils (tex) can be readily observed adhering to the permeate water surface of the RO mem-

brane. The microtopography of the fouling layer generally exhibited a rough-appearing surface texture at low magnification. However, at increasingly higher magnifications (Fig. 8), the outermost aspect of the biofilm on the feedwater surface was found to consist of a complex network of fissures and cavities which invariably harbored large numbers of rod-shaped, filamentous, or coccoid microorganisms. The rod-shaped bacterial cells generally measured 0.3 to 0.5 μm in diameter and about 0.7 to 0.9 μm in length. The bacteria occupying a single microcolony generally looked similar, suggesting that cellular proliferation from a single parental bacterium had occurred in situ. The individual bacteria appeared to be firmly attached by extracellular polymeric fibrils which extended outward from the cell surfaces.

Occasionally, the biofilm was observed in a pseudosagittal (or edgewise) orientation (Fig. 9). In such an orientation, the overall biofilm thickness was readily determined to be from 10 to 20 μm. The biofilm also exhibited a distinct laminar construction in the edgewise orientation. Several individual lamellae composed of bacterial cells compressed to various degrees by the increased hydrostatic pressure were layered upon one another, collectively constituting the biofilm. Usually, three to five such layers were evident within the biofilm, and each layer was on the order of 3 to 5 μm thick. The outermost such layer (on the feedwater surface of the membrane) corresponded to the most recently deposited fouling material and appeared to be the least compacted of the individual lamellae. Organisms of various morphological types were scattered throughout the entire biofouling layer. These bacteria were evidently firmly secured within the biofilm matrix by extracellular fibrillar secretions. It is possible for the observed layering effect of the biofilm to have resulted from the repeated compaction and expansion that occur when the RO facility is shut down and restarted for scheduled maintenance or cleaning. The multilayered construction of the biofilm may also reflect the physico-chemical and microbiological properties of the feedwater entering the RO assembly at different times.

The permeate water surface of the RO membranes was also examined by SEM after removal of the overlying Texlon support fibrils. However, despite an extensive search of this surface, no evidence of microbial colonization was observed. Examination of the outermost exposed surfaces of the polyester Texlon support fibers, on the other hand, did reveal sparse microbial colonization by coccoid, rod-shaped, and filamentous microorganisms (Fig. 10 and 11). The bacteria which were attached to this surface were frequently associated with superficial depressions in the Texlon fiber. The individual cells were attached to the Texlon surface by an extensive network of extracellular fibrillar material. Many of the attached bacteria appeared to have undergone cell division by a transverse fission process, indicating that they were apparently able to proliferate in situ on the Texlon fiber surface (Fig. 11).

(ii) Transmission electron microscopy of fouled membranes. The internal fine structure of the biofilm was examined by transmission electron microscopy of thin-sectioned specimens (Fig. 12 and 13). As in the scanning electron micrographs discussed above, a definite laminar construction for the biofilm is evident in the transmission pictures. The individual biofilm layers were composed primarily of closely packed bacterial cells, many of which appeared to have undergone partial or complete autolytic degeneration. Many of the autolyzed cells were either severely distorted or entirely collapsed, and they had little or no cytoplasmic contents. Large amounts of cytoplasmic membrane material and other envelope debris from completely autolyzed bacteria were observed throughout the biofilm. Embedded within this complex matrix of cellular debris were numerous apparently intact bacterial cells measuring approximately 0.4 to 1.0 μm in diameter. Many of these intact cells were enclosed within a loose network of extracellular polymeric fibrils (Fig. 13) which were presumably used for adhesion or nutrient concentration within the biofilm. Such extracellular fibrils frequently extended outward 0.5 μm or more from the cell surface.

DISCUSSION

Bacteria belonging to the generic groups *Acinetobacter, Flavobacterium-Moraxella, Pseudomonas-Alcaligenes, Bacillus-Lactobacillus, Micrococcus*, and *Serratia* all appear to be involved in biofouling the cellulose diacetate RO membranes used in advanced wastewater treatment at Water Factory 21. However, the ecological role and the extent of involvement of each of these groups in initiating and developing the biofilm are unknown since it is possible that different microbial populations develop on the RO membrane surfaces successively or that seasonal variations occur. Indeed, it is conceivable that one or more of the numerically less significant generic groups detected might predominate at some earlier (or later) stage of biofilm maturation. This possibility is currently being investigated.

The extent to which the findings presented in this paper may be extrapolated to other RO membrane systems has not been ascertained, and there have been few other detailed microbiological investigations of RO biofouling. How-

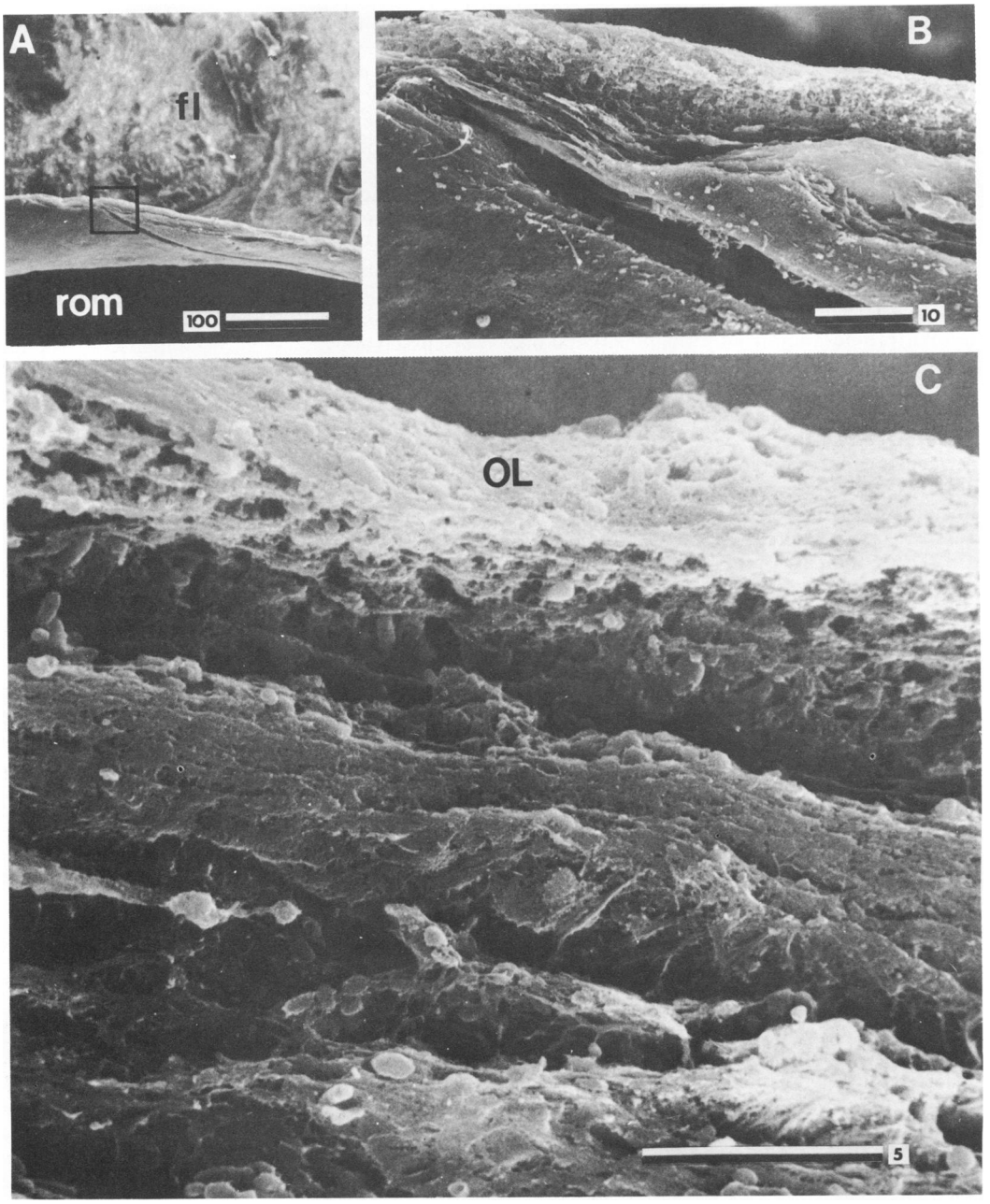

FIG. 9. Scanning electron micrographs of third-pass RO membrane at increasingly higher magnifications showing biofilm in profile orientation. Symbols: fl, feedwater surface of fouling layer; rom, surface of RO membrane; OL, outermost layer of biofilm. Note extracellular fibrillar material and laminar construction of biofilm. Bars, 100 (A), 10 (B), and 5 (C) μm.

ever, it has been demonstrated that many related slime-producing bacteria, including *Pseudomonas* spp. and *Aerobacter* spp., are associated with biofilms which develop on the surfaces of other kinds of RO membranes (2, 3, 22, 29) and recirculating cooling water systems (6, 7, 17, 23, 25, 26). Under laboratory growth conditions, many of the microorganisms isolated from the RO membranes display a readiness to attach to the sides of the culture vessel or to other sur-

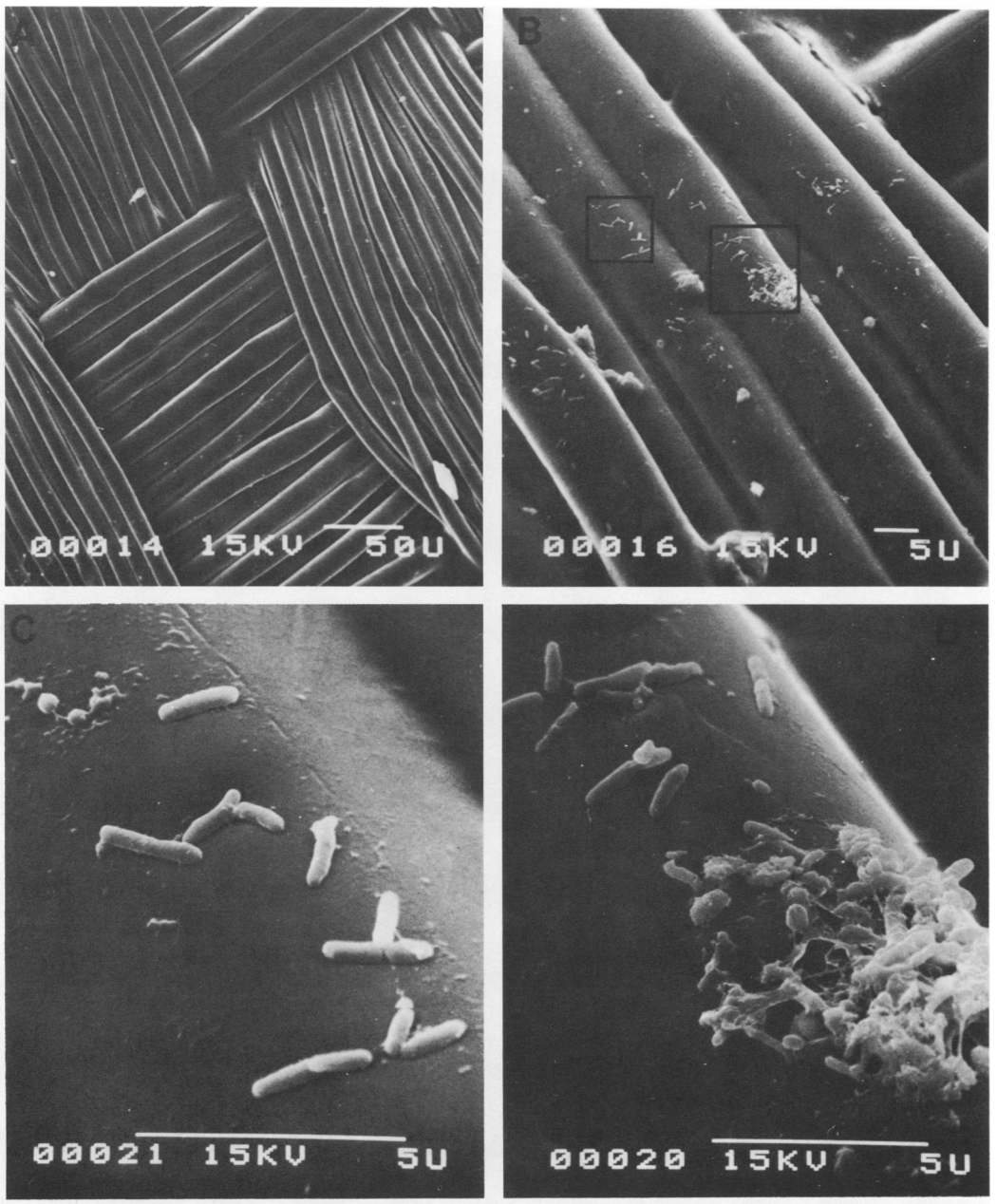

FIG. 10. Scanning electron micrographs at increasingly higher magnifications showing microbial colonization of Texlon support fibers on permeate surface of first-pass RO membrane. Cells appear to be attached to Texlon surface via extracellular fibrillar secretions or stalk-like appendages. Bars, 50 (A) and 5 (B through D) μm.

faces which may be present (unpublished observations). It is tempting to speculate that the adhesive properties of these bacteria may be related to the widespread involvement of such microorganisms in various biofouling processes.

Many of the attached bacterial cells appeared under the electron microscope to be in various stages of cell division by a transverse fission process. This observation, coupled with the presence of ATP and active glucose uptake, strongly suggests that these fouling bacteria were metabolically active on the membrane surfaces. These metabolically active cells have the potential to grow and multiply rapidly under in situ temperature and pressure conditions, utilizing as nutrients other dead bacterial cells associ-

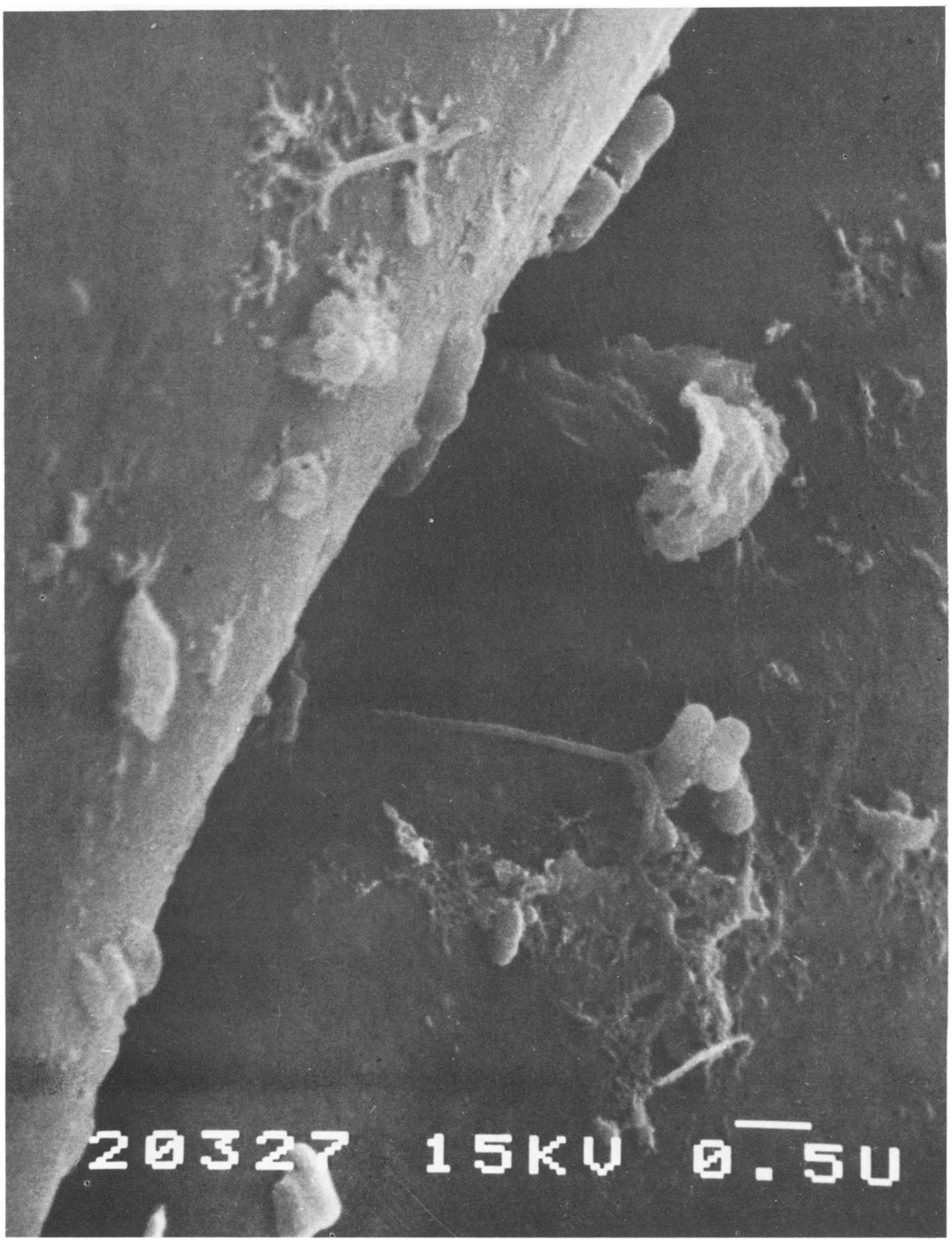

FIG. 11. Scanning electron micrograph showing microbial colonization of Texlon support fiber on permeate surface of third-pass RO membrane. Transverse cross walls are evident in some cells. Note shallow depression on surface of Texlon fiber. Bar, 0.5 μ.

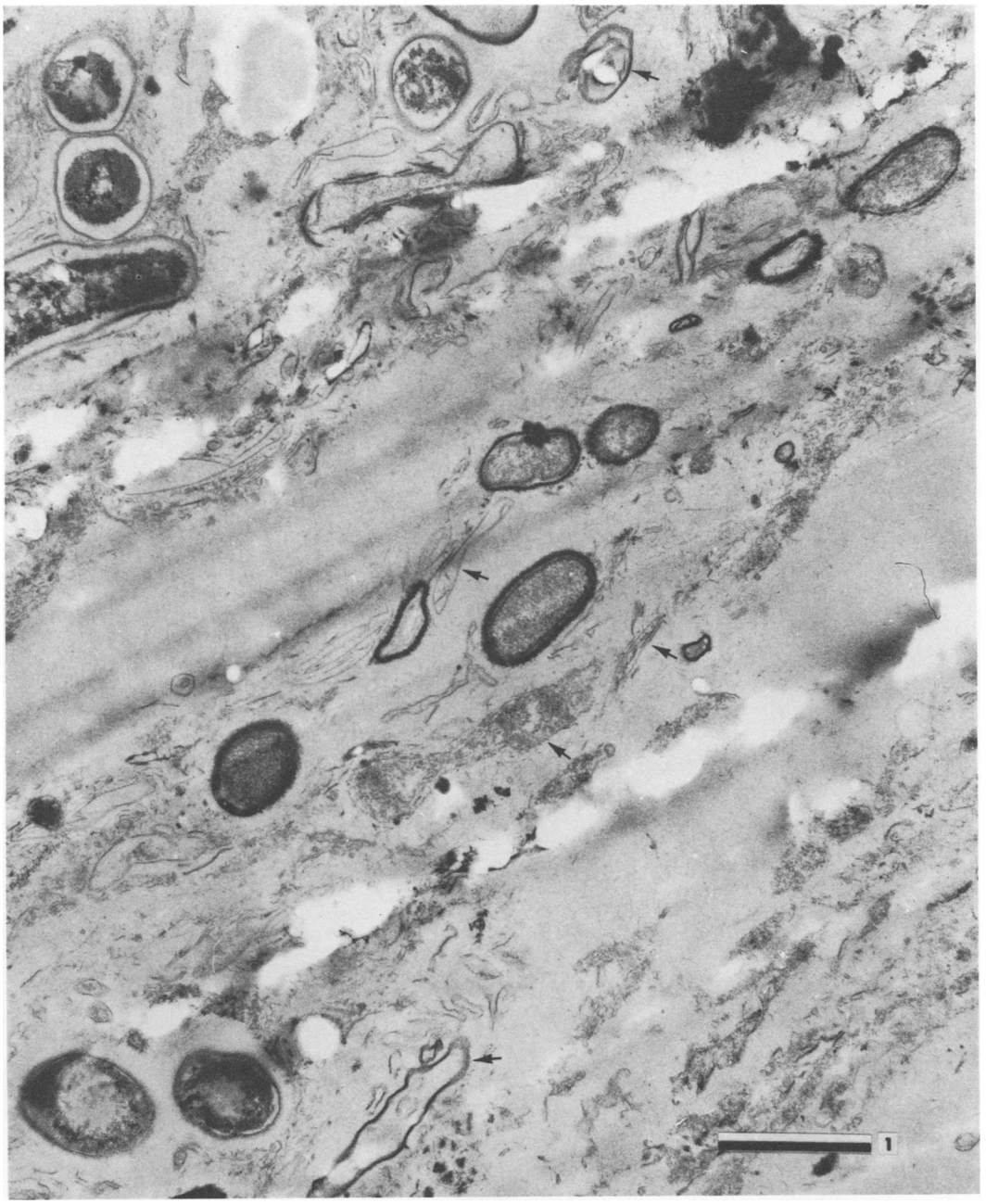

FIG. 12. Transmission electron micrograph of biofilm from second-pass RO membrane. Internal laminar construction of biofilm is evident, as are numerous intact and autolyzed (arrows) bacterial cells. Bar, 1 μm.

ated with the fouling layers or soluble organic nutrients concentrated at the RO membrane surface. Hence, at least two processes appear to be involved in biofilm formation: (i) attachment of microorganisms to the cellulose diacetate membrane surfaces, which may in latter stages of biofilm development be enhanced by physical entrainment, and (ii) cellular growth and proliferation within the biofilm.

The specific physico-chemical and microbiological conditions which prevail on each side of the RO membranes appear to influence the physiological types of microorganisms which eventually become established at each interface.

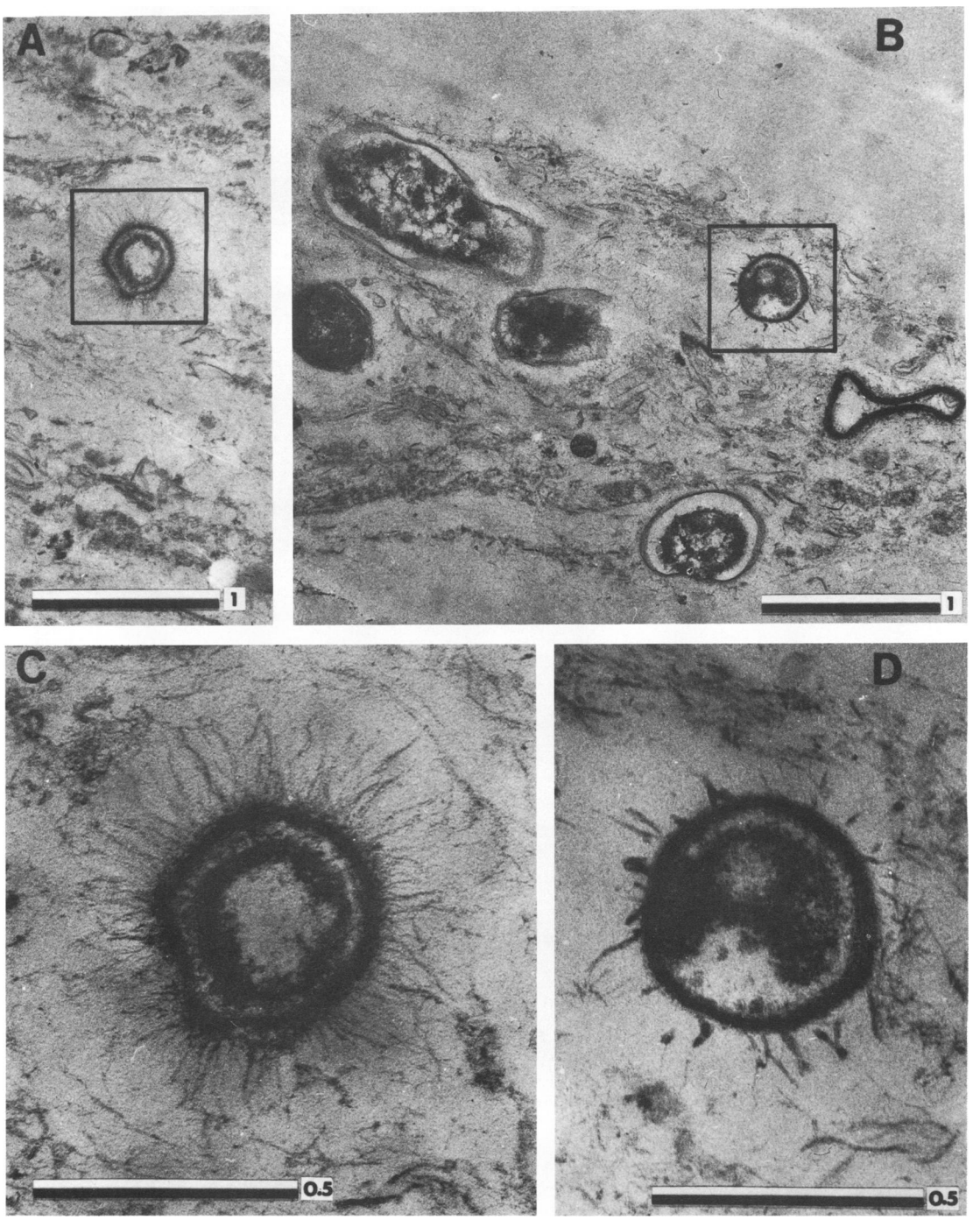

FIG. 13. Transmission electron micrographs of biofilm from second-pass RO membrane. Internal laminar construction of biofilm can be seen in A and B. C and D are enlargements of selected cells showing extruded glycocalyxes consisting of a multitude of extracellular polymeric fibrils. Bars, 1 (A, B) and 0.5 (C, D) μm.

Chemical analyses indicate that the RO feedwater contains approximately 10-fold more total dissolved solids than the permeate water (30, 31). Moreover, because mixing of the feedwater in close proximity to the membrane surface is not absolutely uniform owing partly to the formation of a microbial biofilm and partly to a boundary layer effect (7), inorganic and organic constituents present in the feedwater become even more highly concentrated at the membrane surface (2, 29, 30). Therefore, bacteria attached to the feedwater surfaces of the RO membranes are continually exposed to much greater concentrations of nutrients and dissolved solids than are bacteria on the permeate surfaces. These disparate chemical microenvironments, which are maintained by the innate solute rejection characteristics of the cellulose diacetate semipermeable membranes and the vectorial flow of water through the membranes, may explain the observed differences in microflora on the two sides of the membrane. Hence, the relative increase observed in the *Pseudomonas-Alcaligenes* group of microorganisms on the Texlon fiber surfaces of the RO membranes (compared with the feedwater surfaces) may be related in part to the documented ability of these particular bacteria to survive and proliferate under especially low-nutrient conditions (11).

Bacteria are theoretically physically incapable of passage from the feedwater surface of the RO membrane to the permeate surface. Therefore, microbial colonization of the Texlon support fibers may result from bacterial regrowth within the product water recovery system. In actual practice, however, microorganisms can gain access to the permeate water collection system via small leaks in the rubber O-ring seals which connect adjacent membrane modules or via microscopic holes or other imperfections in the membranes. The adhesion of such waterborne microorganisms to the Texlon fiber surfaces may be prompted by the superficial depressions which were observed in many of the fibers. Attachment of microorganisms in the vicinity of these depressions may be enhanced if local turbulent mixing in such areas is reduced. Localized areas of reduced mixing would effectively increase the duration of contact between a bacterial cell and the Texlon fiber surface, thus allowing more time for irreversible attachment to occur (20, 21).

Although the extracellular fibrils secreted by the attached bacterial cells, as visualized by both SEM and transmission electron microscope analysis, were not chemically analyzed in this investigation, it is reasonable to speculate that these structures consist of acidic mucopolysaccharide or glycoprotein polymers. It has been demonstrated that such biopolymers function in concentrating organic and inorganic trace nutrients at the cell surface (8, 20), as a matrix for the immobilization and activity of specific surface-active extracellular enzymes such as agarase (8, 32) and glucosyltransferase (12), and as extracellular appendages mediating irreversible cellular adhesion to a wide variety of naturally occurring and artificial solid surfaces (5, 8, 15, 20). The extracellular fibrils secreted by the RO fouling microorganisms presumably function similarly to those of bacteria involved in biofouling other kinds of surfaces. Additional studies of the biochemistry, physiology, and molecular genetics of microbial biopolymer synthesis and structure, and of the interaction of these polymers with various solid substrates, may provide the key to improved techniques for controlling microbial adhesion to the RO membranes and other types of industrially important surfaces.

Although bacteria clearly play a central role in the development and maturation of the biofilm, it is unresolved whether a microbial film per se can result in the kind of progressive membrane flux decline that is observed under actual plant operating conditions. Some workers have suggested that membrane water flux decline may instead result from the precipitation of insoluble inorganic (22, 29) or organic (2, 29, 34) substances at the RO membrane surface and that bacteria may be involved only indirectly in a saprophytic capacity. As water is forced through the RO membrane, a wide variety of soluble organic and inorganic compounds normally present in sewage become highly concentrated at the membrane surface, where precipitation may occur. That such chemical precipitation does, in fact, occur to a limited extent at Water Factory 21 is inferred from the increase in inorganic fouling as the feedwater progresses from the first-pass to the third-pass membrane (30, 31). This gradual accumulation of chemical foulants on the membrane surfaces could eventually impede water flux and provide a suitable microenvironment for the adhesion and proliferation of microorganisms. Inorganic fouling of RO membrane surfaces at Water Factory 21, however, does not appear to be a major contributing factor in biofilm genesis or membrane flux decline, although additional experiments will be necessary to define more precisely the roles of various inorganic constituents in the biofouling process. This point should be clarified by experiments currently in progress in this laboratory comparing the temporal kinetics of membrane performance decline with the rate of accumulation of microbial biomass and inorganic substances on the RO membrane surfaces.

ACKNOWLEDGMENTS

The authors thank David G. Argo, Assistant Manager and Chief Engineer, Orange County Water District, for his cooper-

ation and many helpful suggestions. Appreciation is extended to Juta Kiethe, director of the electron microscope facility in the School of Biological Sciences at the University of California, Irvine, for her expert technical assistance with the transmission electron microscope.

This research was supported financially by contract 4107-160-81 from the Orange County Water District.

LITERATURE CITED

1. **American Public Health Association.** 1971. Standard methods for the examination of water and wastewater, 13th ed. American Public Health Association, New York.
2. **Bailey, D. A., K. Jones, and C. Mitchell.** 1974. The reclamation of water from sewage effluents by reverse osmosis. Water Pollut. Control. **74**:353–366.
3. **Besik, F.** 1972. Some aspects of reverse osmosis. Water Sewage Works **119**:76–85.
4. **Buchanan, R. E., and N. E. Gibbons (ed.).** 1974. Bergey's manual of determinative bacteriology, 8th ed. The Williams & Wilkins Co., Baltimore.
5. **Cagle, G. D.** 1975. Fine structure and distribution of extracellular polymer surrounding selected aerobic bacteria. Can. J. Microbiol. **21**:295–408.
6. **Characklis, W. G.** 1973. Attached microbial growths. I. Attachments and growth. Water Res. **7**:1113–1127.
7. **Characklis, W. G.** 1973. Attached microbial growths. II. Frictional resistance due to microbial slimes. Water Res. **7**:1249–1258.
8. **Cheng, K. J., R. T. Irvin, and J. W. Costerton.** 1981. Authochthonous and pathogenic colonization of animal tissues by bacteria. Can. J. Microbiol. **47**:261–290.
9. **Cohen, A. L., D. P. Marlow, and G. E. Garner.** 1968. A rapid critical point method using flourocarbons ("freons") as intermediate transitional fluids. J. Microsc. (Paris) **7**:331–342.
10. **Dubois, M., K. A. Gilles, J. K. Hamilton, P. A. Rebers, and F. Smith.** 1956. Colorimetric method for determination of sugars and related substances. Anal. Chem. **28**:350–356.
11. **Favero, M. A., L. A. Carson, W. W. Bond, and N. H. Petersen.** 1971. *Pseudomonas aeruginosa*: growth in distilled water from hospitals. Science **173**:836.
12. **Gibbons, R. V., and J. van Houte.** 1975. Dental caries. Annu. Rev. Med. **26**:121–136.
13. **Golomb, A., and F. Besik.** 1970. Reverse osmosis—a review of its applications to waste treatment. Water Sewage Works **117**:R-81–R-89.
14. **Hamilton, R. D., and O. Holm-Hansen.** 1967. Adenosine triphosphate content of marine bacteria. Limnol. Oceanogr. **12**:319–324.
15. **Holm-Hansen, O., and C. R. Booth.** 1966. The measurement of adenosine triphosphate in the ocean and its ecological significance. Limnol. Oceanogr. **11**:510–519.
16. **Jones, H. C., I. L. Roth, and W. M. Sanders III.** 1969. Electron microscopic study of a slime layer. J. Bacteriol. **99**:316–325.
17. **Kirkpatrick, J. P., L. V. McIntire, and W. G. Characklis.** 1980. Mass and heat transfer in a circular tube with biofouling. Water Res. **14**:117–127.
18. **Lassen, J.** 1975. Rapid identification of gram-negative rods using a three-tube method combined with a dichotomic key. Acta Pathol. Microbiol. Scand. Sect. B **83**:525–533.
19. **Lowry, O. H., N. J. Rosebrough, A. L. Farr, and R. J. Randall.** 1951. Protein measurement with the Folin phenol reagent. J. Biol. Chem. **193**:265–275.
20. **Marshall, K. C.** 1976. Interfaces in microbial ecology. Harvard University Press, Cambridge, Mass.
21. **Marshall, K. C., R. Stout, and R. Mitchell.** 1971. Mechanism of the initial events in the sorption of marine bacteria to surfaces. J. Gen Microbiol. **68**:337–348.
22. **McCuthan, J. W., and J. S. Johnson.** 1970. Reverse osmosis at Coalinga, California. J. Am. Water Works Assoc. **62**:346–353.
23. **Nickels, J. S., R. J. Bobbie, D. F. Lott, R. F. Martz, P. H. Benson, and D. C. White.** 1981. Effect of manual brush cleaning on biomass and community structure of microfouling film formed on aluminum and titanium surfaces exposed to rapidly flowing seawater. Appl. Environ. Microbiol. **41**:1442–1453.
24. **Reynolds, E. S.** 1963. The use of lead citrate at high pH as an electron-opaque stain in electron microscopy. J. Cell Biol. **17**:208.
25. **Shair, S.** 1971. Microbiocide treatment of recirculating cooling water. Ind. Water Eng. **8**:26–30.
26. **Shair, S.** 1973. Cooling systems defenses against microbiological attack. Power Eng. **77**:68–71.
27. **Shields, P.** 1972. Reverse osmosis for municipal water supply. Water Sewage Works 119:64–70.
28. **Suffet, I. H.** 1980. An evaluation of activated carbon for drinking water treatment: a National Academy of Science report. J. Am. Water Works Assoc. **72**:41–49.

28a. **Taylor, R. E., and E. E. Geldreich.** 1979. Standard plate count methodology: a new membrane filter procedure for potable water and swimming pools. J. Am. Water Works Assoc. **71**:402–405.

29. **U.S. Department of the Interior.** 1979. Reverse osmosis technical manual. Office of Water Research and Technology, U.S. Department of the Interior, Washington, D.C.
30. **U.S. Department of the Interior.** 1979. Evaluation of membrane processes and their role in wastewater reclamation, vol. 1. Office of Water Research and Technology, U.S. Department of the Interior, Washington, D.C.
31. **U.S. Department of the Interior.** 1980. Evaluation of membrane processes and their role in wastewater reclamation, vol. 2. Office of Water Research and Technology, U.S. Department of the Interior, Washington, D.C.
32. **Van der Menlen, H. S., and W. Harder.** 1975. Production and characterization of the agarase of *Cytophaga flevensia*. Antonie van Leeuwenhoek J. Microbiol. Serol. **41**:431–447.
33. **Wechsler, R.** 1976. Reverse osmosis on secondary sewage effluent: the effect of recovery. Water Res. **11**:379–385.
34. **Winfield, B. A.** 1979. A study of the factors affecting the rate of fouling of reverse osmosis membranes treating secondary sewage effluents. Water Res. **13**:565–570.
35. **Winfield, B. A.** 1979. The treatment of sewage effluents by reverse osmosis—pH based studies of the fouling layer and its removal. Water Res. **13**:561–564.